THE JOURNAL OF PHYSICAL CHEMISTRY B LETTERS

2008, *112,* 10777–10781
Published on Web 08/12/2008

Theoretical Third-Order Hyperpolarizability of Paratellurite from the Finite Field Perturbation Method

Mouna Ben Yahia,[†] Emmanuelle Orhan,*[,†] Armando Beltrán,[‡] Olivier Masson,[†] Thérèse Merle-Méjean,[†] Andreï Mirgorodski,[†] and Philippe Thomas[†]

Laboratoire Science des Procédés Céramiques et Traitements de Surface, UMR CNRS 6638, Université de Limoges, 123 av. Albert Thomas, 87060 Limoges Cedex, France, and Departament de Química Fisica i Analítica, Universitat Jaume I, P.O. Box 6029 AP, 12080 Castelló, Spain

Received: June 9, 2008; Revised Manuscript Received: July 18, 2008

Density functional theory was used to estimate the third-order hypersusceptibility $\chi^{(3)}$ of the α-TeO_2 paratellurite (as a model structure for TeO_2 glass) and the same value for α-SiO_2 cristobalite (as a model structure for glassy silica). The attempt was made to gain a physical insight into the nature of the extraordinarily high hypersusceptibility of TeO_2 glass. A finite field perturbation method implemented in the CRYSTAL code with the "sawtooth" approach was employed. The $\chi^{(3)}$ values calculated for α-TeO_2 were found to be of the same order as that measured for TeO_2 glass and much higher than the values computed for α-SiO_2 which, in turn, were close to that of glassy silica.

Although oxide glasses are known to have interesting nonlinear optical properties since the work by Hall et al. in the late 1980s,[1] the origin of this phenomenon is still under debate. As a matter of fact, the wide variety of available techniques for measuring nonlinear third-order susceptibilities can lead to great discrepancies between the measured values for the very same material, mostly related to underestimated error bars. It is thus difficult to compare experiments and to interpret them univocally.[2]

Moreover, theoretical calculations on compounds as disordered as glasses remain tricky and do not allow one to compute physical properties unless the glass is considered not as a whole but as an amount of small molecules. It may not be a problem, since the interesting physical and/or chemical properties of oxide glasses are frequently associated with short-range structural effects. Indeed, oxides are often characterized by typical structural units. For example, vitreous silica and SiO_2-based glasses are built up from a well defined and rigid structural unit, the SiO_4 tetrahedron.

However, this is not the case in TeO_2-based glasses where the "building blocks" are neither so rigid nor so well defined. The tellurite glasses are built up from asymmetrical network formers which are TeO_4 disphenoids (two short and two long bonds), TeO_{3+1} (three short bonds and one long bond), and/or TeO_3 (three short bonds). They are among the most interesting glasses for optoelectronic devices thanks to their high nonlinear susceptibilities, 50 times higher than that of pure SiO_2 glass. Comparative experimental studies completed by *ab initio* calculations on clusters have shown that the TeO_4 structural unit may be responsible for the high third-order susceptibilities.[3,4]

In spite of the theoretical studies carried out in the last five years, the microscopic origin of this property is however still far from final clarity. Localized atomic orbitals have proven the importance of the tellurium lone pair for the high values of microscopic third-order susceptibilities in $Te(OH)_4$ molecules.[5,6] In 2006, a theoretical study carried out on $(TeO_2)_n$ and $(SiO_2)_n$ ($n = 2-12$) clusters in chains, rings, or cage geometries[7] proved that linear chains were the most favorable configuration to achieve high hypersusceptibility values. The polymerization of TeO_2 molecules in chains brought to indices much higher than the addition of each TeO_2 index up to a ceiling of 12 molecules, thus highlighting the influence of collective electronic effects. The results of those studies evidenced the importance of (i) the tellurium lone pair and (ii) a cooperative effect between the TeO_4 entities if they are in a favorable arrangement.

Those methodologies led to interesting elements of thought, but they do not really account for the whole glass structure; they are based on hypothetical fragments that could possibly exist in the glass.

Therefore, relevant information about a stable crystalline structure into which TeO_2 glass finally transforms at heating can be of fundamental interest for a better understanding of these electronic properties at the microscopic level. In this Letter, we propose to obtain the third-order hyperpolarizability coefficients of the stable TeO_2 phase from quantum mechanical *ab initio* calculations.

The paratellurite crystallizes in the P_{41212} space group (#92) with tetragonal symmetry and four formula units per unit cell.[8] There are two independent atomic positions, one tellurium at (x, x, 0) and one oxygen at the general (x, y, z) position. The tellurium first coordination sphere consists in four oxygen atoms in a disphenoidal configuration: a trigonal bipyramid where the third equatorial position is occupied by the tellurium lone pair. The two axial Te−O distances are 2.12 Å, and the two equatorial distances are 1.88 Å. All of the results obtained on α-TeO_2 will be compared to results on SiO_2 for ensuring their validity. The α-SiO_2 cristobalite phase has been chosen rather than α-quartz

* Corresponding author. E-mail: emmanuelle.orhan@unilim.fr.
† Université de Limoges.
‡ Universitat Jaume I.

10.1021/jp805050s CCC: $40.75

TABLE 1: Unit Cell Parameters, Fractional Atomic Coordinates in the Tetragonal P_{41212} Space Group and X−O Distances (X = Te, Si) for α-TeO_2 and α-SiO_2

	α-TeO_2 paratellurite		α-SiO_2 cristobalite	
	experimental[8]	theoretical	experimental[9]	theoretical
a (Å)	4.8082	4.8989	4.9964	5.0285
c (Å)	7.6120	7.7922	7.0125	7.0125
(*x*, *x*, 0)	(0.0268, 0.0268, 0)	(0.02759, 0.02759, 0)	(0.2952, 0.2952, 0)	(0.2992, 0.2992, 0)
(*x*, *y*, *z*)	(0.1386, 0.2576, 0.1862)	(0.1389, 0.2585, 0.1845)	(0.2406, 0.0951, 0.1748)	(0.2396, 0.1039, 0.1784)
X−O distances (Å)	2 × 1.8787	2 × 1.9088	2 × 1.5987	2 × 1.6209
(X = Te, Si)	2 × 2.1212	2 × 2.1604	2 × 1.6057	2 × 1.6204

because it crystallizes in the same space group as paratellurite,[9] with the same independent atomic positions. In the case of cristobalite, the SiO_4 entities are regular tetrahedra and the Si−O distances are all very close to 1.60 Å.

It is important to note that we have no experimental data on the nonlinear susceptibilities of paratellurite and cristobalite crystals. The results will be compared to the values obtained for pure TeO_2 and SiO_2 glasses. Of course, they are not strictly related; the comparison is only interesting in a qualitative way, as both studied crystals contain the local entities meant to be responsible for the nonlinear properties, i.e., TeO_4 and SiO_4.

The response of crystals to external electric fields determines their dielectric behavior, and for computing the nonlinear susceptibilities, derivatives of the total energy with respect to a macroscopic static field are necessary. The main difficulty is the nonperiodic nature of the macroscopic electric potential, meaning that the methods based on Bloch's theorem do not apply. The trick chosen herein to overcome this problem is the use of a "sawtooth" potential in conjunction with a supercell scheme for maintaining the periodicity along the applied field direction, as proposed by Kunc and Resta.[10] In the present work, the finite field sawtooth scheme implemented in the CRYSTAL06 code is used.[11,12] This method, although more expensive in terms of computational power and time than, for example, the variational approach proposed by Souza et al.,[13] has been used successfully for calculating the dielectric constants and the nonlinear indices n_2 of periodic systems.[14,15] By applying the finite field perturbation theory to crystal phases, we aim at gaining insight on the nonlinear optical mechanisms as well as validating the methodology on technologically interesting systems. The *ab initio* calculation of nonlinear coefficient is indeed a very promising substitute of experimental measurements when the quality and/or size of the crystals make them too difficult.

The calculations are performed in the framework of density functional theory (DFT) using Becke's three-parameter hybrid nonlocal exchange functional[16] combined with the Lee−Yang−Parr gradient-corrected correlation functional, B3LYP.[17] The standard B3LYP hybrid method has been extensively used for molecules and also provides an accurate description of crystalline structures with regard to bond lengths, binding energies, and band gap values,[18,19] at least for nonmetallic compounds.[20] The atomic centers have been described by all electron basis sets: 86-311G* for Si,[21] 976631-311G* for Te, and 6-31G* for O. The k-point sampling was chosen to be 18 points in the irreducible part of the Brillouin zone for both cristobalite and paratellurite phases. The number of unit cells in the applied field direction was 6, and 40 points were chosen for the Fourier transform.

Table 1 gathers the geometry optimization results on α-TeO_2 and α-SiO_2 compared to the XRD data. The cell parameters, atomic positions, and distances obtained for α-TeO_2 are in better agreement with experiments than those obtained from plane-wave DFT calculations.[22]

In Figure 1, α-TeO_2 and α-SiO_2 unit cells are represented in order to evidence the similarities between the two structures. Both cations are surrounded by four oxygen atoms in a regular tetrahedron for SiO_4 and a seesaw configuration for TeO_4. The XO_4 (X = Te, Si) polyedra are linked by the corners and form helicoidal chains parallel to *c*.

They also present similarities in their electronic structures. The top of Figure 2 shows the band structures of α-TeO_2 and α-SiO_2, respectively. In both cases, the bands around the forbidden region run sufficiently to indicate the covalent nature of the X−O bonds. An analysis of the bands reveals that both valence bands (VB) are dominated by the 2p states of oxygen atoms, but in the case of TeO_2, the topmost region of the VB is of 2px and 2py character more than 2pz. SiO_2 presents a direct energy band gap of 8.43 eV at Γ point in good agreement with the reported experimental energy gap of 8.4 eV.[23] TeO_2 shows an indirect energy band gap of 4.16 eV between two points belonging to the Γ-M direction, in relative accordance with the value of 3.79 eV measured by Dimitrov and Sakka.[24] The levels forming the bottom of the conduction band are of Si-s, Si-px, and Si-py character for SiO_2 and of Te-px, Te-py, and Te-pz for TeO_2, with the Te-s states being only weakly present.

The bottom of Figure 2 represents the band structures of α-TeO_2 and α-SiO_2 cristobalite under an external electric field of 0.001 au applied in the *z* direction, corresponding to 0.0514 $V \cdot Å^{-1}$. In both cases, all of the levels that were degenerated are now separated. The valence bands become broader with the application of the electric field, and the band gap energies are now 8.16 and 4.05 eV for SiO_2 and TeO_2, respectively. The application of higher electric fields enlarges more the valence bands and causes reduction of the band gaps.

Another way, maybe more intuitive, to explore the effect of an external electric field on the electronic structure is to look at the electron densities. Figure 3 consists of electronic density difference maps between the perturbed and unperturbed electron densities for TeO_2 and SiO_2. The electric field is alternatively applied in the **y** and **z** directions, and the planes chosen for projecting the difference map, always containing one cation and two anions, are taken as parallel as possible to the field direction. It corresponds to the planes materialized by white triangles at

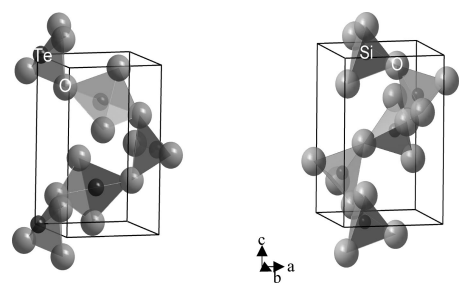

Figure 1. Unit cells for α-TeO_2 paratellurite (left) and α-SiO_2 cristobalite (right).

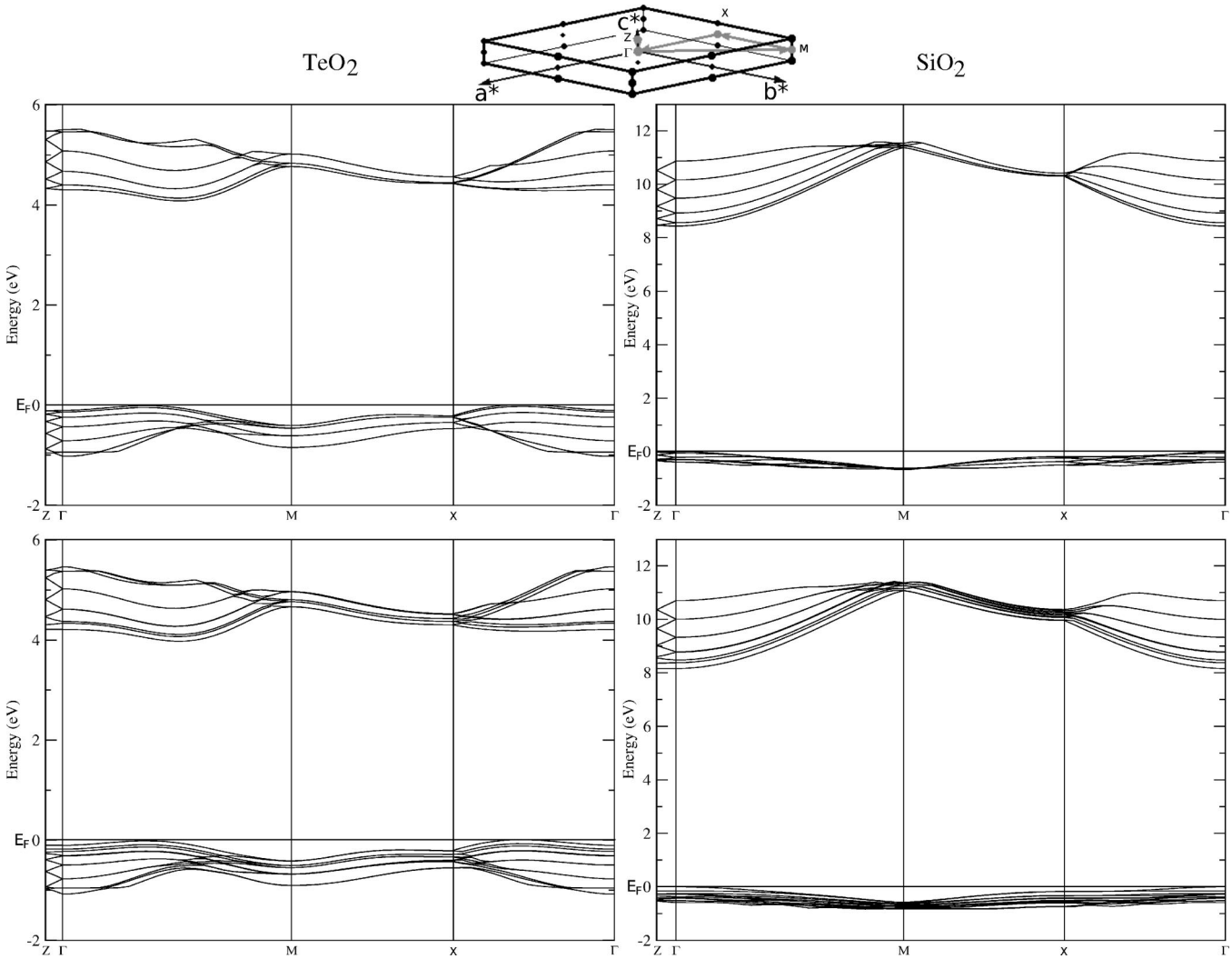

Figure 2. Dispersion of the 10 bands below and above Fermi level for α-TeO_2 paratellurite (left) and α-SiO_2 cristobalite (right) with (bottom) and without (top) an external electric field.

the top of Figure 3. In the case of TeO_2, the plane parallel to **y** contains the axial Te−O bonds (middle left side of Figure 3) and the one parallel to **z** (bottom left side of Figure 3) is the equatorial plane of the TeO_4 disphenoids, containing the Te−O shortest bonds and the tellurium lone pair. In the case of SiO_2, the structure does not allow one to find planes containing two Si−O bonds that are exactly parallel to the cell edges, but they are sufficiently parallel to the applied electric field to give interesting information.

It is visible from the right part of Figure 3 that the oxygen atoms are clearly more polarizable than the silicon, as expected. Deformations of the electronic clouds around the oxygen occupy all of the available space between Si and O. In the case of TeO_2, the electronic cloud around Te is strongly perturbed by the electric field, occupying a large space around the Te position, meaning that the Te lone pair reacts strongly to the field for orientating itself in the field direction as much as permitted by the sterical crowding. When the field is applied along **y**, the lone pair seems to move less than when the field is applied along **z** because it is hampered by the Te−O bond. The effect of the electric field along **y** is thus expected to be less than the effect of the field along **z**. The oxygen atoms are also influenced by the electric field, in the same way as in SiO_2. It is clear that, in TeO_2, the application of an external electric field is sensed not only by the anions but also by the tellurium atoms. The effects on the total polarizability and hyperpolarizabilities are thus conjugated effects of the anion and cation networks.

Table 2 gathers the results concerning the dielectric properties of SiO_2 and TeO_2 both in their crystalline and glassy forms. The calculated linear refractive indices are in very good agreement with the experimental indices. The **z** direction in α-TeO_2 (helicoidal axis) presents a higher index than the **x** and **y** directions, probably because of the greater liberty of the tellurium lone pair in the **z** direction. For α-SiO_2, the linear indices are equivalent in all directions. In Table 2, the third-order susceptibilities are given both in SI units and in the more contested but still in wide use esu-cgs units. To avoid confusion, the susceptibilities are computed in SI and then transformed into esu-cgs units by the formula $\chi^{(3)}$ (SI)/$\chi^{(3)}$ (esu) = $4\pi/(10^{-4}c)^2$, where c is the light velocity in $m \cdot s^{-1}$.[25] As there are no available data on the third-order susceptibilities of the crystalline phases of α-TeO_2 paratellurite and α-SiO_2 cristobalite, the calculated values are compared to the data obtained on glasses with the same composition as the crystal phases. The results seem to be coherent; i.e., the $\chi^{(3)}$ indices calculated for α-TeO_2 are much higher than the indices of α-SiO_2, as for the glass indices. Moreover, the computed values are in the range of the measured ones. For α-TeO_2, the $\chi^{(3)}$ index calculated in the **z** direction (helicoidal chain) is much higher than that in the **x** and **y** directions, probably for the same reason as the linear

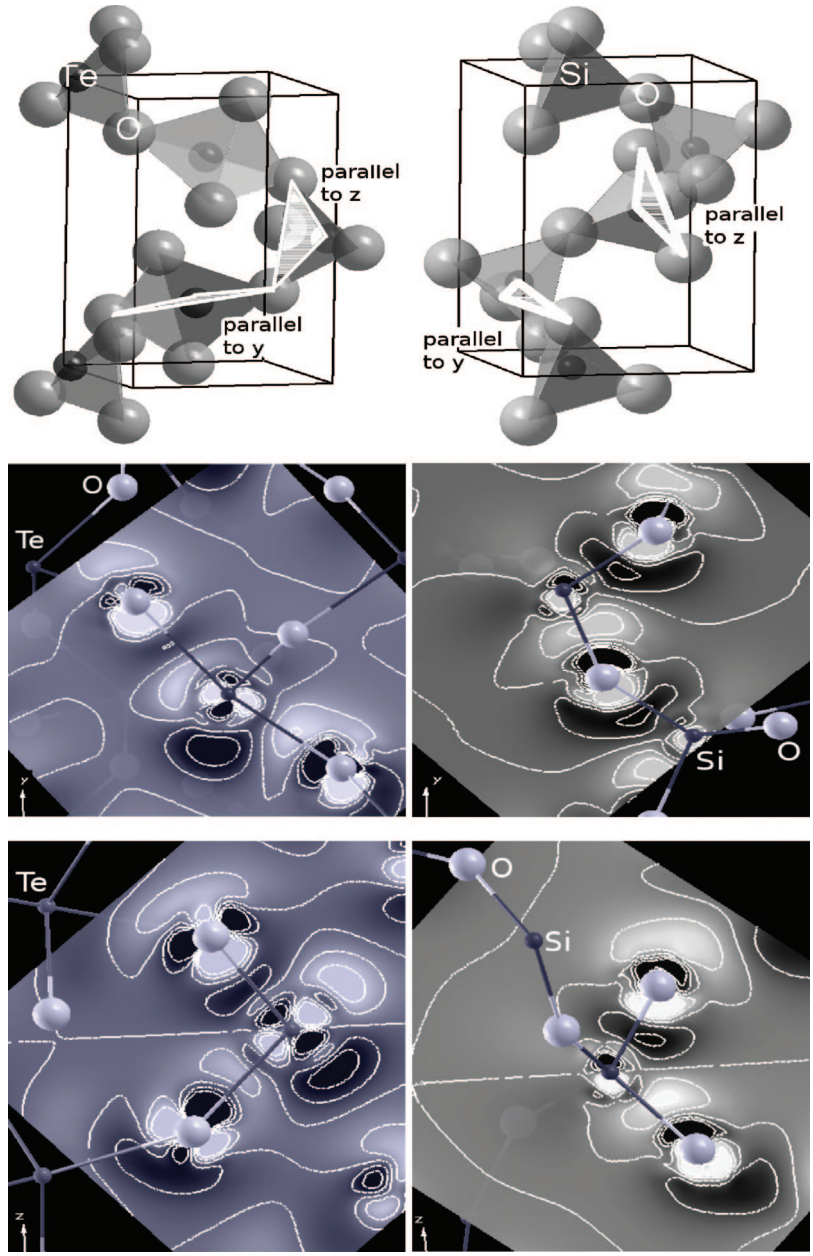

Figure 3. Difference maps between the perturbed and unperturbed electron densities for α-TeO_2 paratellurite (left) and α-SiO_2 cristobalite (right) in planes containing one cation and two oxygens atoms illustrated by the white triangles in the top structures. An electric field of 0.001 au is applied along the **y** and **z** direction. The gray scale ranges from −0.001 to +0.001 e·$bohr^{-3}$.

TABLE 2: Calculated and Measured Optical Properties of TeO_2 and SiO_2 in Their Crystalline and/or Glassy Forms [The Superscripts Indicate the Wavelength of the Measurement (*a*, 633 nm; *b*, 1064 nm; *c*, 1900 nm), and the Values in Bold Come from the Transformation of the esu-cgs Units into SI Units]

	α-TeO_2 (*x*, *y*, *z*) (this work)	exp. α-TeO_2 (*x*, *y*, *z*) TeO_2 glass	α-SiO_2 (*x*, *y*, *z*) (this work)	exp. α-SiO_2 SiO_2 glass
linear refractive index	(2.06, 2.06, 2.25)	(2.20, 2,20, 2,34)[d,26,27] 2.12[c,28]	(1.39, 1.39, 1.39)	1.48[a,23] 1.44[c,28]
$\chi^{(3)}$ (10^{-21} $m^2 \cdot V^{-2}$)	(25.64, 25.64, 44.77)	– **19.68**	(0.73, 0.73, 0.82)	– **0.05−0.39**
$\chi^{(3)}$ (10^{-13} esu)	(18.36, 18.36, 32.07)	– 14.10[c,28]	(0.52, 0.52, 0,59)	– 0.04[b,29]−0.28[c,28]
energy gap (eV)	4.16	3.79[24] 3.37[28]	8.43	8.4[23] 9.0[28]

index. In α-SiO_2, no significant increase of the $\chi^{(3)}$ index in the **z** direction is calculated. So far, our periodic calculations do not allow distinguishing the relative influence of the lone pair (i) from the cooperative effect (ii). The results tend to emphasize that the presence of a free lone pair is necessary to have high nonlinear susceptibilities and that this nonlinear susceptibility is hindered by the sterical crowding, i.e., the atomic arrangement.

In conclusion, the third-order susceptibilities of crystalline α-TeO_2 and α-SiO_2 have been computed for the first time from periodic DFT calculations. The results are in good agreement

with hypersusceptibilities measured on the relevant glasses. Although the origin of the high third-order susceptibilities in TeO_2-based glasses could not be clearly identified from this study, the importance of both the lone pair and the structural environments has been confirmed, in accordance with previous studies from molecular DFT calculations.[5−7] Since the experimental data on crystalline phases are very difficult to obtain, we venture the opinion that this kind of calculation, although technically computer-demanding, could become a powerful prediction tool.

References and Notes

(1) Hall, D. W.; Newhouse, M. A.; Borrelli, N. F.; Dumbaugh, W. H.; Weidman, D. L. *Appl. Phys. Lett.* **1989**, *54* (14), 1293.
(2) Willetts, A.; Rice, J. E.; Burland, D. M.; Shelton, D. P. *J. Chem. Phys.* **1992**, *97* (10), 7590.
(3) Berthereau, A.; Fargin, E.; Villesuzanne, A.; Olazcuaga, R.; Le Flem, G.; Ducasse, L. *J. Solid State Chem.* **1996**, *126*, 143.
(4) Jeansannetas, B.; Blanchandin, S.; Thomas, P.; Marchet, P.; Champarnaud-Mesjard, J.-C.; Merle-Méjean, T.; Frit, B.; Nazabal, V.; Fargin, E.; Le Flem, G. *J. Solid State Chem.* **1999**, *146*, 329.
(5) Suehara, S.; Thomas, P.; Mirgorodsky, A. P.; Merle-Méjean, T.; Champarnaud-Mesjard, J. C.; Aizawa, T.; Hishita, S.; Todoroki, S.; Konishi, T.; Inoue, S. *Phys. Rev. B* **2004**, *70*, 205121.
(6) Suehara, S.; Thomas, P.; Mirgorodsky, A.; Merle-Mejean, T.; Champarnaud-Mesjard, J. C.; Aizawa, T.; Hishita, S.; Todoroki, S.; Konishi, T.; Inoue, S. *J. Non-Cryst. Solids* **2004**, *345*, 730.
(7) Mirgorodsky, A.; Soulis, M.; Thomas, P.; Merle-Mejean, T.; Smirnov, M. *Phys. Rev. B* **2006**, *73*, 134206.
(8) Thomas, P. A. *J. Phys. C* **1988**, *21*, 4611.
(9) Peacor, D. R. *Z. Kristallogr., Kristallgeom., Kristallchem.* **1973**, *138*, 234–298.
(10) Kunc, K.; Resta, R. *Phys. Rev. Lett.* **1983**, *51*, 686.
(11) Dovesi, R.; Saunders, V. R.; Roetti, C.; Orlando, R.; Zicovitch-Wilson, C. M.; Pascale, F.; Civarelli, B.; Doll, K.; Harrison, N. M.; Bush, I. J.; D'Arco, P.; Llunell, M. *CRYSTAL06 User's Manual*; University of Torino: Torino, Italy, 2006.
(12) Rérat, M.; Darrigan, C.; Mallia, G.; Ferrero, M.; Dovesi, R. Crystal Tutorial Project, 2006 (http://www.crystal.unito.it).
(13) Souza, I.; Íñiguez, J.; Vanderbilt, D. *Phys. Rev. Lett.* **2002**, *89*, 117602.
(14) Mallia, G.; Dovesi, R.; Corà, F. *Phys. Status Solidi B* **2006**, *243*, 12.
(15) Darrigan, C.; Rérat, M.; Mallia, G.; Dovesi, R. *J. Comput. Chem.* **2003**, *24* (11), 1305.
(16) Becke, A. D. *J. Chem. Phys.* **1993**, *98*, 5648.
(17) Lee, C. T.; Yang, W. T.; Parr, R. G. *Phys. Rev. B* **1988**, *37*, 785.
(18) Hu, C. H.; Chong, D. P. *Encyclopedia of Computational Chemistry*; John Wiley & Sons: Chichester, U.K., 1998.
(19) Muscat, J.; Wander, A.; Harrison, N. M. *Chem. Phys. Lett.* **2002**, *342*, 397.
(20) Paier, J.; Marsman, M.; Kresse, G. *J. Chem. Phys.* **2007**, *127*, 024103.
(21) Pascale, F.; Zicovitch-Wilson, C. M.; Orlando, R.; Roetti, C.; Ugliengo, P.; Dovesi, R. *J. Phys. Chem. B* **2005**, *109*, 6146.
(22) Ceriotti, M.; Pietrucci, F.; Bernasconi, M. *Phys. Rev. B* **2006**, *73*, 104304.
(23) Weber, J. M. *Handbook of optical materials*; CRC Press: Boca Raton, FL, 2003.
(24) Dimitrov, V.; Sakka, S. *J. Appl. Phys.* **1996**, *79*, 1741.
(25) Butcher, P. N.; Cotter, N. *The Elements of Nonlinear Optics*; Cambridge University Press: Cambridge, U.K., 1990.
(26) Uchida, N. *Phys. Rev. B* **1971**, *4* (10), 3736.
(27) Okada, M.; Takizawa, K.; Leiri, S. *J. Appl. Phys.* **1977**, *48* (10), 4163.
(28) Kim, S.-H.; Yoko, T.; Sakka, S. *J. Am. Ceram. Soc.* **1993**, *76* (10), 2486.
(29) Adair, R.; Payne, L. L. *J.Opt. Soc. Am. B* **1987**, *4*, 875.

JP805050S